Electronic Supplementary Material (ESI) for Catalysis Science & Technology.

The role of acid and metal sites in hydrodeoxygenation of guaiacol over Ni/Beta catalysts

Penghui Yan,[†] Molly Meng-Jung Li,[†] Eric Kennedy,[†] Adesoji Adesina,[‡] Guangyu Zhao,[†] Adi Setiawan,[§] and Michael Stockenhuber*[,†]

[†]Chemical Engineering, School of Engineering, The University of Newcastle, Callaghan, NSW, 2308, Australia

[‡]Atodatech LLC, Camarillo, California 93010, United States

[§]Mechanical Engineering, Faculty of Engineering, Universitas Malikussaleh, Bukit Indah, Lhokseumawe, 24352, Indonesia

***Corresponding author:** michael.stockenhuber@newcastle.edu.au

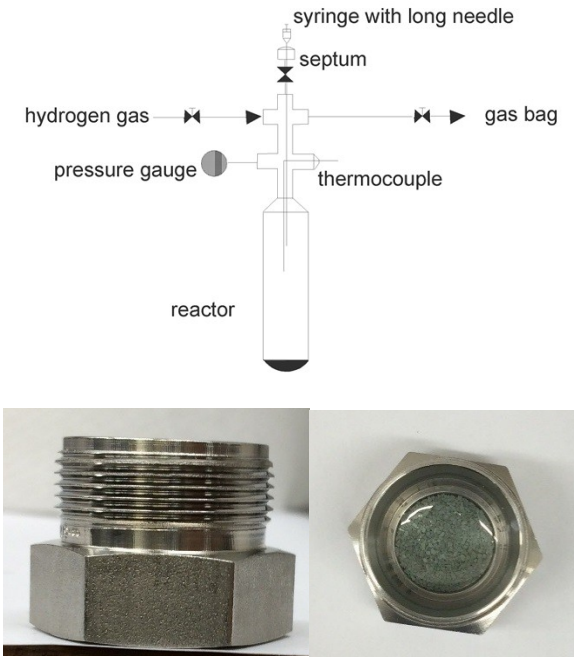

Figure S1. Experimental set up and photo of the mixed state of catalyst and feed (cap diameter: 3/4 inch, 0.2 g catalyst, 0.4 g guaiacol)

Mass-transfer limitations

The hydrodeoxygenation of guaiacol on the reduced Ni/BEA catalyst surface involves transfer of hydrogen into liquid phase and diffusion through the liquid phase to the catalyst through a boundary layer surrounding the catalyst surface. To investigate the intrinsic

activity of the catalyst, the internal mass transfer were examined by using two different particle sized catalyst, the external mass transfer limitations were checked by using different mass of catalyst but keep the same WHSV and GHSV. In addition, the mass transfer limitations were also examined by means of the Weisz-Prater (C_{WP}) and Mears Criterion (C_M) [1]. Both the experimental and calculation results show the hydrodeoxygenation under the employed reaction conditions is not limited by the mass transfer (internal mass transfer and external mass transfer).

Table S1. HDO of guaiacol over Ni/BEA catalyst with different particle size[a]

Catalyst (23.2 wt% Ni/BEA-12.5)	X-guaiacol (%)	Y-cyclohexane (%)	Others (%)
250~450 μm	15.7	6.2	9.4
450~600 μm	15.1	5.8	7.8

[a] Reaction conditions: H_2 (4.0 MPa), WHSV (3.12 min^{-1}), catalyst mass 0.05 g, H_2 flow rate (120 mL/min)

Table S2. HDO of guaiacol over Ni/BEA catalyst with different catalyst mass[a]

Catalyst (23.2 wt% Ni/BEA-12.5)	X-guaiacol (%)	Y-cyclohexane (%)	Others (%)
33.3 mg	15.2	6.5	7.5
50.0 mg	15.1	5.8	7.8
62.5 mg	14.8	6.0	8.0

[a] Reaction conditions: H_2 (4.0 MPa), WHSV (3.12 min^{-1}), GHSV (1500 min^{-1}), catalyst particle size (450~600 μm)

Calculation of Weisz-Prater Criterion and Mears Criterion

The detailed calculations for the Weisz-Prater Criterion and Mears Criterion are presented below.

(1) The absence of mass transport resistances was checked by Weisz-Prater Criterion (C_{wp}) for internal diffusion and Mears Criterion (C_M) for external diffusion, respectively.

$$C_{WP} = \frac{r_{obs}\rho_c R_P^2}{D_{eff} C_S}$$

$$C_M = \frac{r_{obs}\rho_b R_P n}{k_c C_{Ab}}$$

Where r_{obs} is observed reaction rate, mol kg^{-1} s^{-1}; n is the reaction order; R_P is the catalyst particle radius, m; ρ_c is the bulk density of catalyst bed, kg m^{-3}; ρ_b is the bulk density of catalyst bed, kg m^{-3}, $\rho_b=(1-\varepsilon)\rho_c$; ε is porosity; C_S is liquid concentration of guaiacol at the external surface of the catalyst, mol m^{-3}; C_{Ab} is liquid concentration of guaiacol, mol m^{-3}; k_c is the external mass transfer coefficient, m s^{-1}.

In this work, a H_2 gas flow rate of 120 mL min^{-1}, a catalyst particle size of 0.25-0.50 mm.

For the Ni/BEA catalyst,

R_P=(250+500)/2=187 um=1.87 × 10^{-4} m, n=1,

ε=0.72, $R_{guaiacol}$=4.06 × 10^{-2} mol·kg^{-1}·s^{-1}, ρ_b=0.625 × 10^3 kg·m^{-3},

ρ_c=2.23 × 10^3 kg·m^{-3},

$C_S \approx C_{Ab}$=4875 mol·m^{-3},

the reaction liquid density, ρ=1.11 × 10^3 kg·m^{-3}, the reactor inner diameter, 4.57 × 10^{-3} m, the reactant flow rate, 7.2 mL·h^{-1}, viscosity, μ=3.129 × 10^{-5} Pa·s

fluid velocity $u=\frac{7.2\times10^{-6}}{3600\times3.14\times(2.28\times10^{-3})^2}=1.22\times10^{-4}\ m\ s^{-1}$

$D_{AB}=9700r\sqrt{\frac{T}{M}}=9700\times8.0\times10^{-7}\times\sqrt{\frac{503}{128}}=1.53\times10^{-2}\ cm^2\ s^{-1}$

$D_{eff}\approx D_{AB}$=1.53 × 10^{-6}·m^2 s^{-1}

The external mass transfer coefficient is calculated below.

$$\frac{Sh\varepsilon}{1-\varepsilon}=(\frac{R_e}{1-\varepsilon})^{1/2}Sc^{1/3}$$

$$\frac{k_cR_p}{D_{AB}}\left(\frac{\varepsilon}{1-\varepsilon}\right)=\left[\frac{\rho uR_p}{\mu(1-\varepsilon)}\right]^{1/2}\left(\frac{\mu}{\rho D_{AB}}\right)^{1/3}$$

$$\frac{\rho uR_p}{\mu(1-\varepsilon)}=\frac{1.11\times10^3\times1.22\times10^{-4}\times1.87\times10^{-4}}{3.129\times10^{-5}(1-0.72)}=2.9$$

$$\frac{\mu}{\rho D_{AB}}=\frac{3.129\times10^{-5}}{1.11\times10^{-3}\times1.53\times10^{-6}}=0.01842$$

$$\frac{k_cR_p}{D_{AB}}\left(\frac{\varepsilon}{1-\varepsilon}\right)=\frac{k_c\times1.87\times10^{-4}}{1.53\times10^{-6}}\left(\frac{0.72}{1-0.72}\right)=2.9^{1/2}\times0.01842^{1/3}=1.7\times0.264$$

obtained, k_c = 1.43 × 10^{-3} m·s^{-1}

Therefore,

$$C_{WP}=\frac{R_{guaiacol}\rho_cR_P^2}{D_{eff}C_S}=\frac{4.06\times10^{-2}\times2.23\times10^3\times(1.87\times10^{-4})^2}{1.53\times10^{-6}\times4875}=0.0004244<1$$

$$C_M = \frac{R_{guaicol}\rho_b R_P n}{k_c C_{Ab}} = \frac{4.06 \times 10^{-2} \times 0.625 \times 10^3 \times 1.87 \times 10^{-4} \times 1}{1.43 \times 10^{-3} \times 4875} = 0.0006806 < 0.15$$

Generally, according to the Weisz-Prater Criterion and Mears Criterion, when the calculation value for C_{WP} and C_M is below 1 and 0.15, respectively, the internal and external diffusion limitations can be neglected during the kinetic experiments. The C_{WP} and C_M are 0.0004244 and 0.0006806, respectively, under the above experimental conditions, suggesting that the internal and external diffusion limitations could be neglected during the kinetic experiments. Therefore, the reaction rate could be used to represent the intrinsic activity of the catalysts.

Analysis of heat transfer effects

The radial heat transfer effect was estimated by the Mear criterion (C_{MH}) [2] which is defined by the following equation:

$$C_{MH} = \left| \frac{-\Delta H\,(-r)(1-\varepsilon)R^2}{\lambda T(1+b)} \right| < 0.4\frac{RT}{E_a}$$

Where ΔH is heat of reaction, r is observed reaction rate, R is the inner radius of the tubular reactor, ε is the catalyst bed porosity, and the λ is the effective thermal conductivity of porous catalyst, b is the ratio of diluent to catalyst volume, and the R is the gas constant.

$C_7H_8O_2 + 5H_2 = C_6H_{12} + H_2O + CH_3OH$

$\Delta H_f C_7H_8O_2$=-307.95 kJ/mol, $\Delta H_f H_2$=0 kJ/mol, $\Delta H_f C_6H_{12}$=-156.4 kJ/mol, $H_f H_2O$=-241.8 kJ/mol, $H_f CH_3OH$=-201 kJ/mol

$\Delta H = \Delta H_f(\text{products}) - \Delta H_f(\text{reactants})$=-291.25 KJ

ε= 0.72

r= 4.06 × 10^{-2} mol/kg· s = 25 mol/m^3·s

R= 4.57 × 10^{-3} m

λ= 0.1 W/m·K [3],

b= 0

T=503 K

E_a= 40.279 kJ/mol (calculated based on Arrhenius equation)

$$\left| \frac{-\Delta H\,(-r)(1-\varepsilon)R^2}{\lambda T(1+b)} \right| = \frac{291.25 \times 25 \times (1-0.72) \times (4.57 \times 10^{-3})^2}{0.1 \times 503 \times 1} = 8.46 \times 10^{-4}$$

$$0.4\frac{RT}{E_a} = 0.4 \times \frac{8.314 \times 503}{40279} = 0.0415$$

The calculation results showed that the C_{MH} was 2 orders of magnitude lower than the $0.4\frac{RT}{E_a}$, therefore, radial heat-transfer effect in the HDO reaction was not a factor.

Table S3. Textural properties of reduced and used catalysts

Sample	T-Plot Micro pore area[a] (m^2/g)	T-Plot mesopore surface area[a] (m^2/g)	Pore volume[b] (cm^3/g)	T-plot micropore volume[a] (cm^3/g)	Average pore size[b] (nm)	D_{Ni}[c] (%)
Beta-12.5	315	207	0.37	0.17	8.1	-
Beta-25	277	192	0.34	0.15	8.8	-
Beta-175	312	191	0.12	0.17	4.0	-
Reduced 15.7 wt% Ni/Beta-12.5	243	147	0.29	0.15	8.6	6.7
Reduced 23.2 wt% Ni/Beta-12.5	229	139	0.31	0.12	9.6	4.6
Reduced 15.7 wt% Ni/Beta-25	221	124	0.26	0.13	8.6	8.6
Reduced 15.7 wt% Ni/Beta-175	257	123	0.09	0.15	4.1	3.7
ZSM-5-15	198	129	0.11	0.09	4.6	-
Reduced 15.7 wt% Ni/ZSM-5(Si/Al=15)	170	66	0.06	0.10	5.1	-

[a] calculated by t-plot method;

[b] calculated by BJH adsorption theory (1.7 ~300 nm);

[c] Calculated by chemisorption, dispersion of Ni was calculated by assuming a stoichiometry of CO/Ni=1/1.

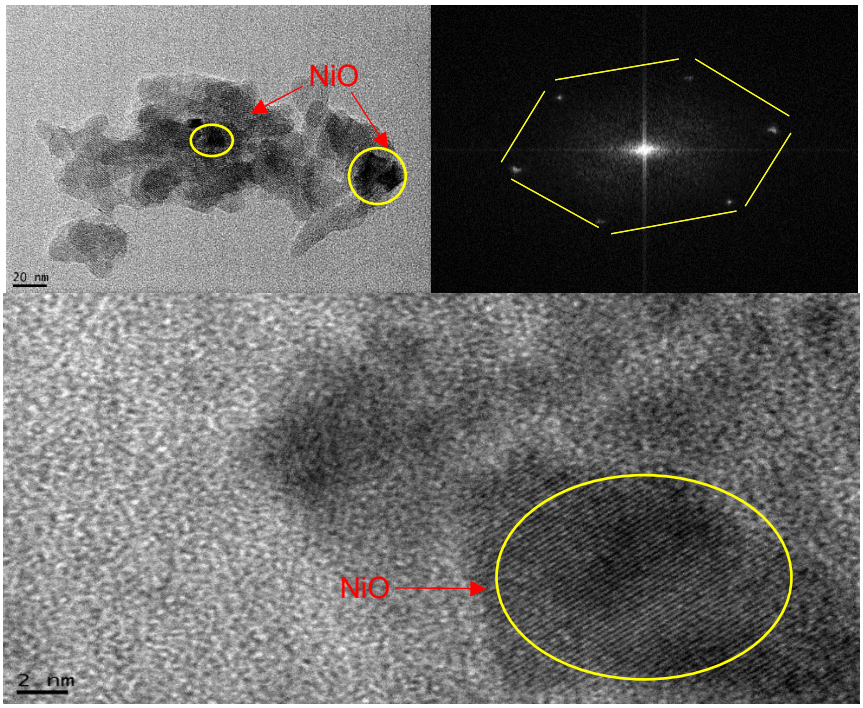

(**a**)

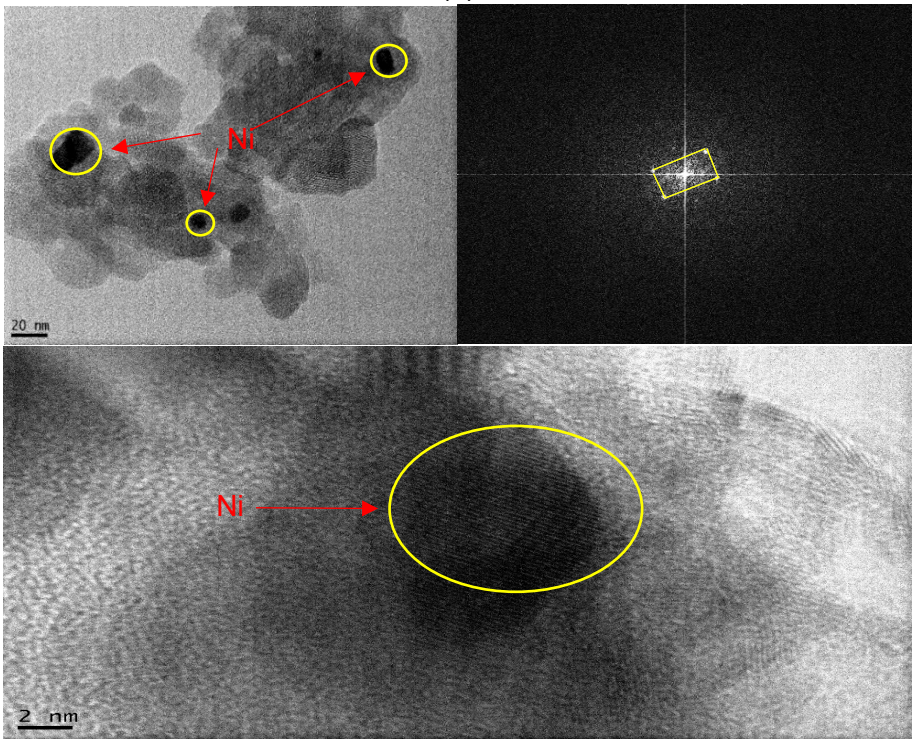

(**b**)

Figure S2. TEM of calcined (a) and reduced (b) 15.7 wt% Ni-Beta-12.5 catalyst

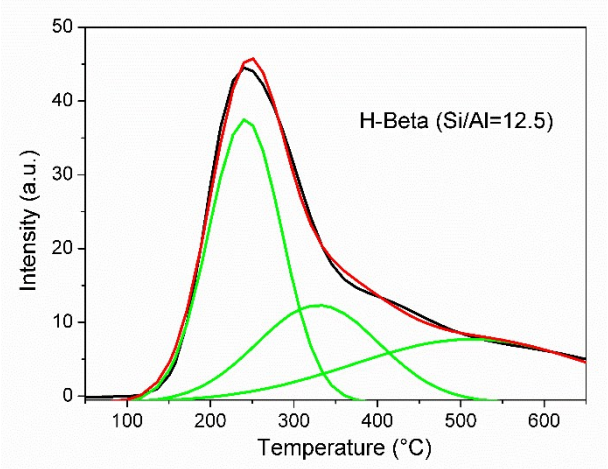

Figure S3. Ammonia temperature programmed desorption profile of H-Beta-12.5 zeolite, m/z=16, the black line - original trace, the red line - the composite sum of fitted peaks, and the green line - fitted peaks

Table S4. Estimated heats of desorption of calcined Ni/Beta catalysts

Catalyst	Peak	T_{max}[a] (K)	ΔE_{des}[b] (kJ mol^{-1})
15.7 wt% Ni-Beta-12.5	LTP	493	123.7
	MTP	563	141.9
	HTP	712	180.9
15.7 wt% Ni-Beta-25	LTP	492	123.5
	MTP	575	145.0
	HTP	688	174.6
15.7 wt% Ni-Beta-175	LTP	528	132.8
	MTP	645	163.3

[a] Temperature at peak maxima of desorption from NH_3-TPD; [b] Heat of ammonia desorption, $\frac{\Delta E_{des}}{RT_{max}} = ln\frac{v1T_{max}}{\beta}$ -3.64, v_1=10^{13} s^{-1}

Table S5. Acid characterization of parent Beta and reduced Ni-based catalysts measured by IR spectra of adsorbed ammonia[a]

Sample	Acid sites determined by NH_3-FTIR (mmol/g)	
	Brønsted	Lewis
HBeta-12.5	0.81	0.24
HBeta-25	0.71	0.10
HBeta-175	0.25	0
reduced 15.7 wt% Ni/Beta-12.5	0.60	0.56
reduced 15.7 wt% Ni/Beta-25	0.50	0.49
reduced 15.7 wt% Ni/Beta-175	0.26	0.09

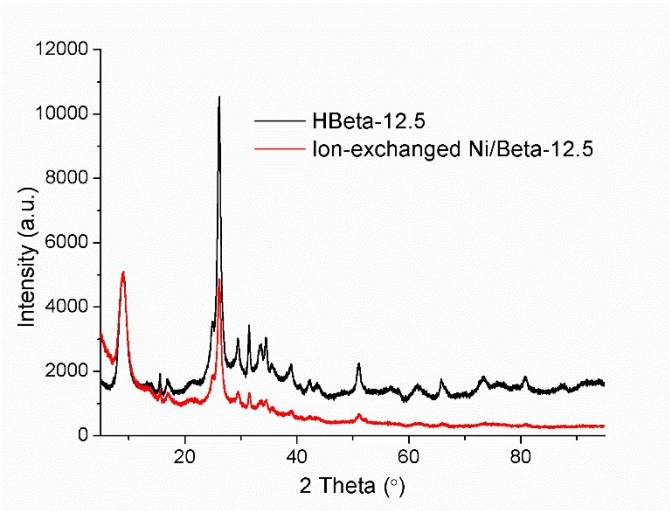

Figure S4. XRD patterns of HBeta-12.5 and ion-exchanged Ni/Beta-12.5 samples

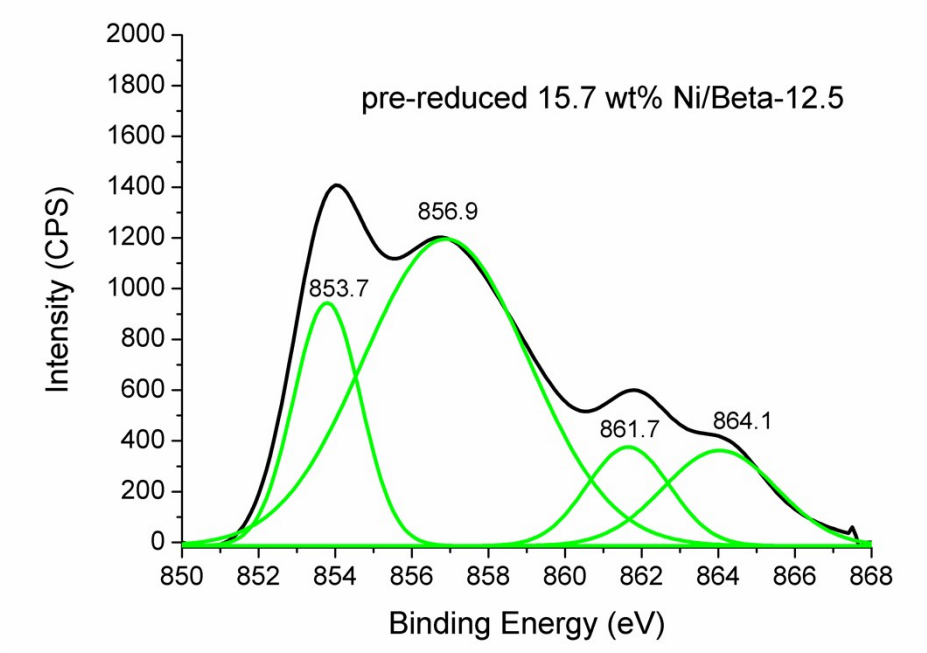

Figure S5. XPS of pre-reduced 15.7 wt% Ni/Beta-12.5 sample

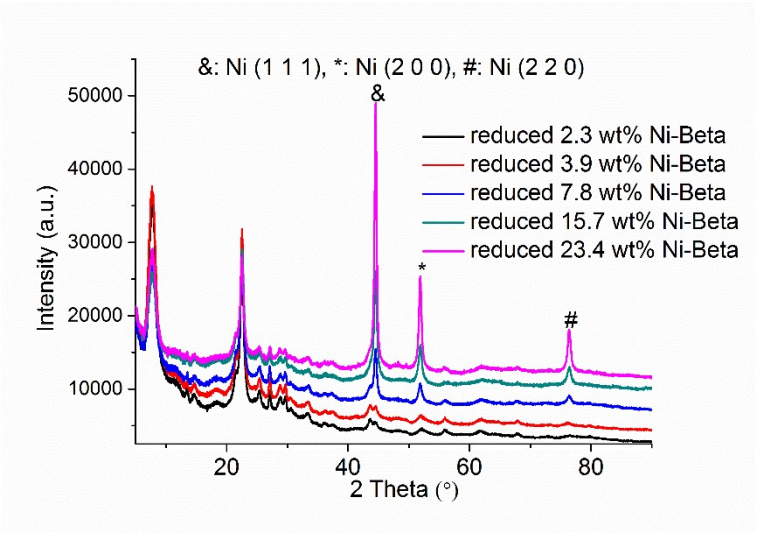

Figure S6. XRD patterns of reduced Ni/Beta-12.5 samples

Table S6. The performance results of HDO of guaiacol over Ni/Beta-12.5 and supports using a continuous flow reactor[a]

Chemicals	Catalysts					
	Ion-exchanged Ni/Beta-12.5	2.3 wt% Ni/Beta-12.5	HBeta-12.5	HBeta-25	HBeta-175	Al_2O_3
Conversion (%)	19.5	23.4	14.9	13.9	11.7	17.8
Methylcyclopentane (%)	0.46	0	0	0	0	0
Cyclohexane (%)	0.75	0	0	0	0	0
Cyclohexene (%)	0.57	0	0	0	0	0
Toluene (%)	0.33	0.45	0	0	0	0
Anisole (%)	0.41	0.46	0.21	0	0	0
Phenol (%)	0.68	0.68	0.12	0	0	0
p-Cresol (%)	0.77	0.56	0.46	0.42	0.39	0.40
2,6-Dimethylphenol (%)	0.12	0.13	0.10	0.10	0.10	0.08
1,2-Dimethoxybenzene (%)	4.58	5.00	3.45	3.20	3.88	0.44
2-Methoxy-6-methylphenol (%)	1.58	2.11	1.36	0.87	1.19	1.15
2-Methoxy-5-methylphenol (%)	0.98	1.31	0.99	0.60	0.83	0.07
Creosol (%)	1.09	1.49	0.90	0.14	0.77	0.43
Catechol (%)	3.57	6.85	4.71	4.31	4.10	5.42
4-Ethyl-2-methoxy-phenol (%)	0	0	0	0	0	0.27
2,3-Dimethoxytoluene (%)	0.18	0.15	0.07	0	0.07	0.07
3-Methyl-1,2-benzenediol (%)	0.66	1.39	0.82	0.53	0.32	2.67
4-Methyl-1,2-benzenediol (%)	0.49	1.10	0.62	0.31	0.28	0.06

4-Ethyl-2-methoxyphenol (%)	0.15	0.23	0.09	0	0.06	0
2,5-Dimethyl-1,4-benzenediol (%)	0.22	0.44	0.16	0	0	1.75
2,5-Dimethoxytoluene (%)	0.09	0.18	0.07	0	0	0
4,5-Dimethy-1,3-benzendiol (%)	0.11	0	0	0	0	0.12
2,3,4,6-Tetramethylphenol (%)	0	0.22	0	0	0	0.14
2,3,5-Trimethyl-1,4-benzenediol (%)	0.07	0.11	0.05	0.27	0.23	0.46
2-Isopropyl-1-methoxy-4-methylbenzene (%)	0.11	0.14	0	0	0	0.42

[a] Reaction conditions: WHSV (0.26 min^{-1}), reaction temperature (300 °C), catalyst (0.1 g), guaiacol (0.026 g/min), 4.0 MPa H_2, H_2 flow rate (120 mL/min).

Reference

[1] W.Q Fu, L. Zhang, D. F. Wu, M. Xiang, Q. Zhuo, K. Huang, Z. D. Tao, T. D. Tang, J. Catal. 330 (2015) 423

[2] D. E. Mears, Ind. Eng. Chem. Process Des. Dev. 10 (1971) 541

[3] N. Joshi, A. Lawal, Ind. Eng. Chem. Res. 52 (2013) 4049